IEEE Access
Multidisciplinary | Rapid Review | Open Access Journal

Received 28 April 2022, accepted 11 May 2022, date of publication 23 May 2022, date of current version 21 November 2022.

Digital Object Identifier 10.1109/ACCESS.2022.3177208

Cooperative Active Power Management in Multifrequency Microgrid With an Energy Storage System Based on Distance of Source to Load

RAJDIP DEY, (Student Member, IEEE), AND SHABARI NATH, (Member, IEEE)
Department of Electronics and Electrical Engineering, Indian Institute of Technology Guwahati, Guwahati 781039, India
Corresponding author: Rajdip Dey (rajdip.dey@iitg.ac.in)

ABSTRACT A multifrequency microgrid (MFMG), which has different frequency voltages and currents on the multifrequency (MF) bus can be constructed based on the superposition theorem, orthogonal power flow theory, and frequency selective power transmission criteria. It is a unique system where different frequency powers are present on the bus and all active powers maintain orthogonality by flowing simultaneously through a conductor without mixing. Due to the uncertainty and intermittency of renewable sources, an energy storage system (ESS) needs to be installed with MFMG to maintain stability and reliability. The ESS will be charged/discharged based on different frequency active power imbalances in the MF bus. Due to the presence of different frequency voltages and currents on the MF bus, the integration of ESS with MFMG is challenging but not yet discussed in any literature. In this paper, an architecture of MFMG is proposed with ESS. It is found that different new power imbalance cases arise in MFMG due to different frequency sources and loads, which are not present in traditional microgrids. Here, active power balancing conditions for all power imbalance cases are defined for grid connected and islanded modes. An algorithm is proposed to coordinate the ESS and different renewable sources to balance different frequency active power demands in MFMG for optimum power generation through communication under a cooperative framework. The framework is created based on the assumption that any load prefers to take power from the nearest source to minimize the power loss and cost. Different source load pairs are categorized based on the physical distance by different frequencies and accordingly the algorithm is structured. Finally, a Matlab simulation of a sample 9 bus MFMG is performed to validate the algorithm and all results are presented.

INDEX TERMS Active power management, DC/MF converter, energy storage system, frequency selectivity power flow, multifrequency microgrid, power imbalance case, orthogonal power flow, source-load pair.

NOMENCLATURE

Subscripts:

S, L	Source, Load variables.
diff , *var*	Difference between load and source side variables.
b	Multifrequency bus variables.
G	Grid variables.
GF	Grid forming converter variables.
GFE	Grid feeding converter variables.
GI	Grid interactive converter variables.
$BESS$	Battery variables.
F	Filter variables.
B	Capacitor bank variables.
f	Frequency.
e	Error.
ref	Reference value of variables.
T	Total value of variables.
new	New value of variables in changed condition.
av	Maximum available value of variables.

Symbols:

P_{b-f-S}	Total f^{th} frequency source power at MF bus.
P_{b-f-L}	Total f^{th} frequency load power at MF bus.

The associate editor coordinating the review of this manuscript and approving it for publication was Ehab Elsayed Elattar.

$P_{b-f-diff}$	Total f^{th} frequency power difference at MF bus.
P_{Lx}	Load power of x^{th} bus.
P_{Sx}	Source power of x^{th} bus.
P_{Sx-f}	f^{th} frequency power segment of source power of x^{th} bus.
$P_{Sx-BESS}$	Source power segment of x^{th} bus for battery.
P_{BESS-f}	f^{th} frequency battery power segment.
V_{b-f}	f^{th} frequency voltage at MF bus.

Acronyms:

DL	Domestic load.
EV	Electric vehicle.
ESS	Energy storage system.
GI	Grid interactive.
GCF	Gain crossover frequency.
IL	Industrial load.
MFMG	Multifrequency microgrid.
MF	Multifrequency.
MT	Micro turbine.
PID	Proportional integral derivative.
PV	Photo voltaic.
PWM	Pulse Width Modulation.
SOC	State of charge.
SOH	State of health.
TF	Transfer function.
WT	Wind turbine.

I. INTRODUCTION

The current power system confronts several new challenges related to load growth, quality of power, and integration of renewable sources. Microgrid solves these problems by connecting the local loads with renewable sources without major construction and can support the main grid by active and reactive power to improve power quality [1]. A microgrid can be operated in grid connected or islanded mode depending upon the availability of the grid [2]. To increase the reliability and stability of microgrids, different types of storage systems are integrated [3].

Multiple frequency elements are overlapped on the MF bus of MFMG as shown in Fig. 1. MFMG is formed based on three basic concepts named superposition theorem, orthogonal power flow theory, and frequency selectivity criteria [4]. This system permits several independent load source interactions to occur simultaneously on a single transmission line with different frequency channels. Orthogonal active power flow theory conveys that if two elements in a circuit are tuned to a certain frequency which is different from the rest of the system then they can create an active power channel without hampering other elements of the system [5]. Several active power channels can be created on a single conductor if different frequency elements are employed. At the load side, each active power channel can be identified and users can consume power selectively from the desired channel or source [6]. MFMG has multiple other advantages and new features over conventional microgrids. As multiple operational frequencies

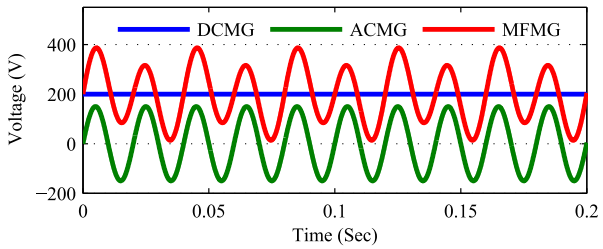

FIGURE 1. Bus voltage of DC, AC and Multifrequency microgrid [4].

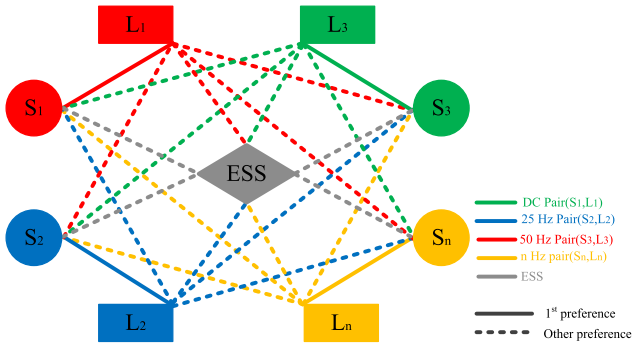

FIGURE 2. Coordinated power management architecture of MFMG.

are present on the MF bus, decoupled power control can be implemented which gives a higher degree of flexibility and functionality [7]. In the modern power system, the number of DC loads is increasing rapidly. System efficiency is increased in MFMG by omitting the AC/DC transformation which is required for DC loads [8]. Transmission capacity is increased without changing the thermal capacity of the conductor by superimposing different frequency currents on the same wire keeping the voltage level same [9]. Different power companies can send different types of power categorized upon source-load distance, cost, reliability, availability, and power quality through multiple frequency channels present on the MF bus. The MFMG load side converter has the ability to convert any other frequency available active power of the MF bus to load frequency active power. So MFMG loads can consume several frequency active powers simultaneously from the MF bus. Due to this unique advantage, for any MFMG a new power market can be designed where different active powers are differentiated by using different frequency channels. Without any new construction, a more competitive power market structure can be formed [6]. For this firstly, a proper different frequency active power balancing strategy is needed for the MFMG system.

In this paper, the MFMG architecture is formed based on the assumption that all sources and loads are connected by a single MF bus and each load prefers to take power from the nearest source to reduce the power loss and cost. If the nearest source power is not available then it can take the excess power from all other available sources equally so that loads can be operated in extreme situations. Each load-source pair is operated in a distinctive frequency to differentiate that pair

from rest of the system. As all sources and loads of MFMG are connected by power electronic converters, this operation is possible irrespective of the source and load frequency. The MFMG power management architecture is presented in Fig. 2. In this structure S_1 and L_1 are operated as DC pair, S_2 and L_2 are operated as 25 Hz pair and similarly, S_n and L_n are operated as 'n' Hz pair. The logic behind the power management is that the DC load (L_1) should take power from the DC source (S_1). If DC source power is not available then DC load will take power from other sources ($S_2, S_3, \ldots S_n$) equally. An ESS is added to this MFMG to increase the stability and reliability of the system. If total source power ($\sum_{f=1}^{n} P_{f-S}$) is higher than total load power ($\sum_{f=1}^{n} P_{f-L}$) then the ESS will be charged and if total load power is higher than total source power then ESS will be discharged and maintain the active power balance in extreme conditions. If this strategy is implemented in a traditional microgrid for 'n' number of sources and 'm' number of loads then a total ($m * n$) number of dedicated connections need to be constructed. For MFMG, only one MF bus can connect all the sources and loads to reduce the installation and maintenance cost of the system.

The MFMG structure which is proposed in [4], does not contain any ESS unit. The addition of ESS gives several advantages and drawbacks to the MFMG system which are not covered in any literature. The integration and operation of ESS with MFMG are challenging as different frequency active powers are present on the MF bus. A proper power management strategy needs to be defined for ESS to maintain the state of charge (SOC) level. An active power exchange strategy between the ESS, different frequency sources, and loads need to be proposed.

The architecture [4], converter [8], control strategies [4], [10] of MFMG are already defined. ESS can provide voltage and frequency support by storing/delivering active power during peak supply/load scenarios in a microgrid [11]. ESS increases the stability and reliability of the system by providing power balance in extreme conditions [12]. The integration strategy of ESS with AC [13], DC [14], and Hybrid [15], [16] microgrids are proposed in several works of literature but the operation of ESS with MFMG is still not explained in any literature. As MF bus contains different frequency active powers so several new active power imbalance cases happen by ESS integration which are not observed in any traditional microgrid. All active power imbalance cases need proper investigation and power balancing criteria need to be defined for all cases. Considering all active power balancing criteria, a proper active power balancing algorithm should be proposed.

The major contributions of this paper are:

- An MFMG architecture is proposed with three different frequency sources, loads, and ESS. The control strategy of the ESS is explained to supply different frequency active powers.
- Different new active power imbalance cases which occur due to the integration of ESS with MFMG are properly discussed and the active power balancing conditions for all these cases are defined.
- Based on the power balancing conditions, a cooperative active power balancing algorithm is proposed for MFMG with an ESS for both grid connected and islanded modes.
- The performance analysis of the algorithm is done by simulating a 9 bus MFMG in the Matlab Simulink environment for different power imbalance cases.

In this paper, a proper literature review on the different MF systems and active power control strategies of conventional microgrids with ESS are conferred in Section II. The active power imbalance problem of MFMG, different new active power imbalance cases, and power balancing conditions for islanded and grid connected modes are examined in Section III. An algorithm is proposed to balance different frequency active powers of MFMG with ESS for different power imbalance cases in Section IV. The algorithm is verified by simulation and all simulation results are shown in Section V. Section VI concludes the paper.

II. LITERATURE REVIEW

Recently several researchers are working on the multifrequency system due to its unique nature which needs to be highlighted. ESS becomes an integral part of the microgrid system due to several advantages. The recent work on the MF system and integration of ESS with traditional microgrids are listed here.

A. LITERATURE ON MF SYSTEM

The superposition of DC and 50 Hz AC was first narrated in [9] and the current and voltage limit were calculated for each frequency. In modular multilevel converter [5], and distributive power flow converter [17], the 50 Hz and its third harmonic are separately controlled to achieve two different functions. A smart transformer is proposed in [7] to attain MF power transfer in a distribution system. The basic design and concept of load side converter are conferred in [10], where the converter behaves like a power filter to create frequency selective power transmission in the MF system. The hardware realization of the load converter is presented in [18] and how the consumer can choose any frequency available power from the MF bus is explained. The architecture and converters of an MFMG are presented in [8]. The operation of the DC/MF converter is explained in [6] as grid feeding, forming, and load side converter of MFMG.

B. LITERATURE ON ESS

Research work regarding ESS integration and management to a microgrid is emerging in recent years. Different energy storage systems like battery [19], flywheel [20], and superconducting magnetic energy storage [21] are already reported in the literature. In [22], [23] the size of ESS is optimized considering reliability and resilience. Different control strategies like centralized [24], cooperative [13], [25], [26], coordinated [27], [28], PID controller based [29], [30], and

TABLE 1. Comparison of proposed strategy with existing literature.

References	[14], [15], [24], [31].	This work.
Bus voltage frequency	50 Hz (AC) [24, 31], DC [14], 50 Hz and DC (Hybrid) [15].	DC+ 25 Hz+ 50 Hz (MF).
Active Power imbalance case	Two cases for AC or DC [24, 31, 14], and four cases for hybrid microgrid [15].	Eight cases for MFMG.
Active power balancing strategy	Centralized d-q power control in [24], fuzzy logic control in [31], positive and negative sequence components control in [14],V-F control in [15].	Centralized d-q power control.
Active power sharing strategy	Based on cost in [14], based on source rating [15].	Based on distance between source and load to reduce active power loss and cost.
Converter control strategy	Inverter current control in [24], fuzzy control in [31], Combined feedforward and feedback control in [14], and droop control in [15].	Voltage mode and average current control.
Source side power categorization	Not possible.	Source side powers can be categorized depending upon their availability, reliability, cost, or distance of the source from load and pass through different frequency power channels of MF bus without mixing.
Consumer power selection	Not possible.	Consumers have the ability to choose between different frequency powers from MF bus based on their needs.

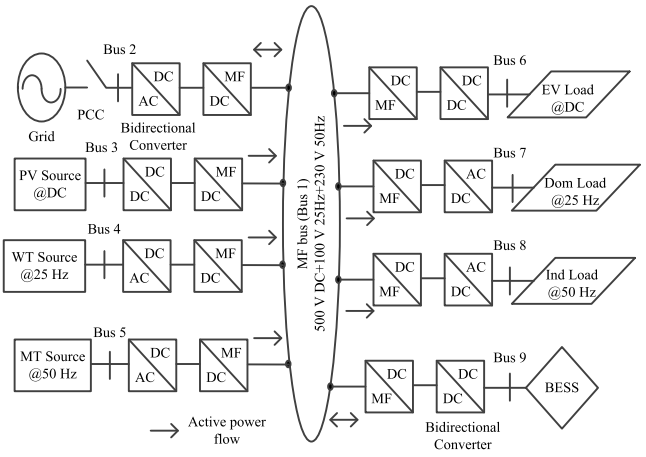

FIGURE 3. Architecture of MFMG with ESS.

fuzzy logic control [31] are reported to manage the active power of AC microgrid with ESS. Different distributed [14] and droop based [32] power sharing algorithms for ESS and DC microgrid are proposed. The controlled architecture of a hybrid microgrid with ESS is explained in [33]. In [15], an autonomous power control strategy is described for hybrid microgrid and ESS. For a cluster of microgrids and an ESS, a cooperative power control strategy is proposed in [34], [35]. There is no literature that discuss the architecture and control of MFMG with ESS. Next, a well-defined power balancing algorithm of different frequency active powers is needed for MFMG with ESS. To understand the innovative contributions of the paper with respect to the state-of-the-art, a comparison table is presented in Table 1.

III. ACTIVE POWER BALANCE PROBLEM OF MFMG WITH ESS

The functioning of a microgrid primarily depends on its architecture. First, the architecture of the MFMG with ESS is introduced here. Based on the architecture, different active power imbalance cases are investigated for grid connected and islanded modes.

A. ARCHITECTURE OF MFMG

Unlike hybrid microgrid, MFMG has only one bus (MF bus) where different frequency voltages are superimposed. The connection of MF sources, loads, and ESS to MF bus is presented in Fig. 3. Here, 0 Hz (DC), 25 Hz, and 50 Hz are chosen as the base frequency of the architecture. All different frequency sources and loads are connected to the MF bus by power electronic converters based on the operating frequency of the source or load. The grid is connected to bus 2 by an AC/DC and DC/MF converter. The MF bus (bus 1) voltage is chosen as $500V\ DC+100V\ 25Hz+230V\ 50Hz$. One 100 kW photovoltaic (PV) unit acts as the DC source in bus 3 and is connected by a DC/DC and DC/MF converter. Two wind turbines (WT) of 80 kW are chosen as 25 Hz sources in bus 4 and connected by an AC/DC and DC/MF converter. One of the WT's converters behaves like a grid interactive converter. A 60 kW microturbine (MT) consists of a turbine and synchronous generator that behaves like a 50 Hz source at bus 5 and is integrated into the MF bus by AC/DC and DC/MF converter. All source data are taken from [36], [37], and [38]. The closest load of the DC source is EV at bus 6. So the EV load is operated as a DC load and connected by an MF/DC to DC/DC converter. In the same way, the industrial load (IL) at bus 7 acts as a 50 Hz load and the domestic load (DL) at bus 8 behaves like a 25 Hz load. The IL and DL are non-sensitive loads and load shedding can be done. The domestic load becomes almost double in grid connected mode as the grid interactive source can supply the required active power. A lithium-ion battery is chosen as the ESS due to higher energy density, higher voltage capacity, and longer life, and it is connected to bus 9. The rating of the battery energy storage system (BESS) is 50 kW, 375 V, 0.8 kAh for 6 $Hour$. The BESS is connected to the MF bus by a DC/DC bidirectional converter and DC/MF converter.

B. PROBLEM OF ACTIVE POWER BALANCE WITH ESS

Total active power supply and consumption should match with each other in any electrical system to maintain the frequency and stability of the system bus. A consumer in the MFMG can choose any accessible frequency power from the MF bus. With frequency selective active power transmission, different active power imbalance situations are created which are not present in traditional AC, DC, or hybrid microgrid. From the architecture, it can be noticed that the MF bus contains three different frequency active powers. In a traditional microgrid only one frequency source or load is present but in this MFMG, three different frequency (DC, 25 Hz, 50 Hz) sources and loads are present. So several new active power imbalance cases are evolved. In MFMG, all sources are connected by power electronic interfaces. So any frequency source power can be converted to required other frequency power and sent to the MF bus. For any source-load pair if the load power is higher then other available sources can generate extra power to balance that load. To balance different frequency active powers first, the active power

difference of each source-load pair needs to be calculated. Accordingly, different active power imbalance cases are formed. For proper operation of MFMG and ESS, a different frequency active power control and management algorithm is necessary which should balance all active power imbalance cases. In this paper, active power control problems are examined separately for islanded and grid connected modes.

1) ISLANDED MODE

MFMG needs to be self-supported in terms of power in islanded mode. Here the grid interactive converter behaves like a grid forming converter and controls the MF bus voltage. The different frequency active powers of MFMG are controlled by grid feeding converters and ESS. For traditional DC and AC microgrids with ESS, the condition for active power balances are given in equation (1, 2). In a traditional microgrid, the ESS power is equal to the difference between the source and load power of that frequency.

$$P_{ESS} = P_{b-0-S} - P_{b-0-L} \tag{1}$$

$$P_{ESS} = P_{b-50-S} - P_{b-50-L} \tag{2}$$

In MFMG, the DC/MF converters are able to convert any frequency active power to other frequency active power so one single ESS unit can store different frequency active powers by proper power conversion. Equation 3 presents the active power balancing criteria for an MFMG system with ESS which states that the ESS power should be equal to the difference between the algebraic sum of different source and load powers. ESS side DC/MF converter has the ability to convert the ESS power to required difference active powers and vice versa. Accordingly, if total source power is higher than load power then the ESS is charged and if total load power is higher than the total source power then ESS is discharged.

$$P_{ESS} = \sum_{f=1}^{n} P_{b-f-S} - \sum_{f=1}^{n} P_{b-f-L} \tag{3}$$

For an MFMG with three different frequency (DC, 25 Hz, 50 Hz), the active power balance condition is,

$$P_{ESS} = P_{b-0-S} + P_{b-25-S} + P_{b-50-S} - P_{b-0-L} - P_{b-25-L} - P_{b-50-L}$$

As all sources of MFMG are connected to power electronic converters so any frequency source side active power can be converted to other frequency active power and the source converter sends that to the MF bus as per load demand. The source-load pair active power differences are presented in equation (4) [39]. So the ESS power should be equal to the different source-load pair active power differences.

$$P_{b-f-diff} = P_{b-f-L} - P_{b-f-S} \quad \text{for } f = DC, 25, 50 \tag{4}$$

$$P_{ESS} = \sum_{f=1}^{n} P_{b-f-diff} \quad \text{for } f = DC, 25, 50 \tag{5}$$

Based on different source-load pair active power differences, several new active power imbalance situations occur in MFMG. In this paper, a sample MFMG is chosen (Fig. 3), for which the active power balancing algorithm needs to be defined. Total three source-load pairs are there and they are operated in DC (PV, EV), 25 Hz (WT, DL), and 50 Hz (MT, IL) frequency. The active power balance problem of an MFMG without the ESS is already discussed and for three frequencies (DC, 25, 50), total of six power imbalance cases are defined in [39]. Here, it has been found that with the power support of ESS, active power balance can be possible for two more imbalanced cases where previously power balance was not possible. A table (Table 2) is formed with the previously shown six cases (Case2 - Case7) [39] and two new cases (Case1, Case 8), which may occur in the islanding condition of MFMG with ESS. For all these eight cases active power balancing strategy should be different and accordingly, the algorithm needs to be designed.

From the table, it can be seen that the Case 1 has imbalance situation of $P_{b-0-diff} = 0, P_{b-25-diff} = 0, P_{b-50-diff} = 0$. For this situation, all different frequency loads in MFMG are balanced by their paired sources. Still, the sources need to produce extra power to charge up the BESS. Case 4 has a power imbalance condition of $P_{b-0-diff} = 0, P_{b-25-diff} = 0, P_{b-50-diff} > 0$. Here DC and 25 Hz active power pairs are balanced. The 50 Hz source reaches its maximum limit and still cannot deliver the 50 Hz load power. So for this case, the available sources (DC, 25 Hz) should produce extra DC and 25 Hz active power equally. Source side converters will convert those powers to the required 50 Hz active power ($P_{b-50-diff}$) and send that to the MF bus to maintain the active power balance of the total system. For Case 8, the imbalance condition is $P_{b-0-diff} > 0, P_{b-25-diff} > 0, P_{b-50-diff} > 0$. Here all sources of MFMG are at their maximum available value, yet can't fulfill the paired load demand. Here the excess load power is produced by the ESS and different frequency active powers got balanced. These two cases (case 1, case 8) are not reported in any literature and accordingly, the power balancing algorithm needs to be modified.

For islanded mode, a new control strategy is required where

- The MF bus voltage will be maintained by the grid interactive converter.
- If total source power is higher than total load power then ESS will be charged and the different source-load pair active power mismatches will be supplied by other frequency sources.
- If total source power is lower than total load power then ESS will be discharged and the different source-load pair active power mismatches will be supplied by other frequency sources and ESS.

2) GRID CONNECTED MODE

In this mode, the grid controls the MF bus voltage. As the price of storage power is higher than grid power, so the ESS is never discharged in grid connected mode. The lithium-ion battery should be operated in mid-SOC which is $20\% - 80\%$

TABLE 2. Different cases of active power imbalance in islanded mode of the MFMG with ESS [39].

Case 1	$P_{b-0-diff} = 0, P_{b-25-diff} = 0, P_{b-50-diff} = 0$
Case 2	$P_{b-0-diff} > 0, P_{b-25-diff} = 0, P_{b-50-diff} = 0$
Case 3	$P_{b-0-diff} = 0, P_{b-25-diff} > 0, P_{b-50-diff} = 0$
Case 4	$P_{b-0-diff} = 0, P_{b-25-diff} = 0, P_{b-50-diff} > 0$
Case 5	$P_{b-0-diff} > 0, P_{b-25-diff} = 0, P_{b-50-diff} > 0$
Case 6	$P_{b-0-diff} > 0, P_{b-25-diff} > 0, P_{b-50-diff} = 0$
Case 7	$P_{b-0-diff} = 0, P_{b-25-diff} > 0, P_{b-50-diff} > 0$
Case 8	$P_{b-0-diff} > 0, P_{b-25-diff} > 0, P_{b-50-diff} > 0$

for longer life and to maintain a good state of health [40]. The ESS will only be charged in grid connected mode and if SOC reaches 80% then the ESS will be disconnected. Here, the main objective of the developed control is to set the active power reference of grid in a way that it balances all source-load pair active power mismatches and charge the ESS. The grid side converter converts the 50 Hz grid power to different frequency required active powers and sends those to MF bus for active power balance of MFMG. The active power balance equation for grid connected mode is,

$$P_G = \sum_{f=1}^{n} P_{b-f-diff} + P_{ESS} \tag{6}$$

In this paper, the grid need to balance three different frequency source-load pairs (DC, 25 Hz, 50 Hz) in the MFMG. So the active power balancing condition becomes,

$$P_G = P_{b-0-diff} + P_{b-25-diff} + P_{b-50-diff} + P_{BESS} \tag{7}$$

For grid connected mode, a new control strategy is required where,

- The MF bus voltage will be maintained by the grid and grid interactive converter behaves like a grid feeding converter.
- Different source-load pair active power differences and battery power will be supplied by the grid.
- ESS will be charged and disconnected when SOC reaches 80%.

IV. PROPOSED CONTROL ALGORITHM TO MAINTAIN THE BALANCE OF DIFFERENT FREQUENCY ACTIVE POWERS IN MFMG WITH ESS

In this section, a cooperative active power balancing algorithm is explained to balance different frequency active power imbalances for grid connected and islanded modes. The cooperative frame is formed based on the assumption that each load prefers to take power from its nearest source.

A. COOPERATIVE ALGORITHM FOR ACTIVE POWER BALANCE

An algorithm for cooperative control of the sources of MFMG is proposed under varying different frequency loads for grid connected and islanded modes. The logic behind the algorithm is that each load takes active power from its paired source. If the active power of that pair is still not balanced, then the load absorbs power from other available sources equally. For islanded mode, if $P_{b-f-diff} = 0$, then that source-load pair active power is balanced and the source is available to generate more active power if required. If $P_{b-f-diff} > 0$, then that source-load pair active power is not balanced, and to balance active power that load takes power from other available sources equally. In grid connected mode if $P_{b-f-diff} > 0$, then that pair load takes the required power from the grid and the different frequency active powers of the MFMG get balanced. The ESS is only charged in grid connected mode. In islanded mode, if $P_{ST} > P_{LT}$ then ESS takes the extra source power to store. If $P_{LT} > P_{ST}$ then ESS discharges and supplies the required load active power. The flowchart for the proposed algorithm is conferred in Fig. 4. There is a total of ten steps are there in the algorithm. The algorithm works for both grid connected and islanded modes. The main steps of the algorithms are,

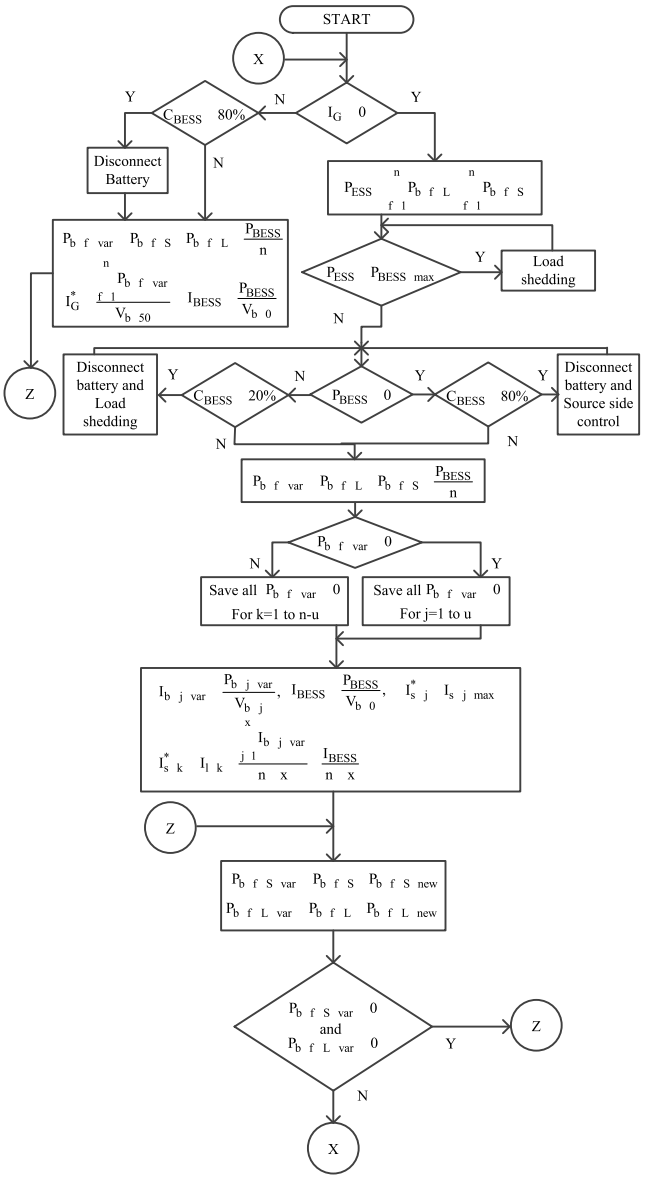

FIGURE 4. Different frequency active power balancing flowchart for MFMG with ESS.

- Step 1: Check MFMG is operated in islanded mode or grid connected mode -

$$I_G = 0 \begin{cases} Yes & \text{Then islanded mode confirmed and goto step 4.} \\ No & \text{Then grid connected mode confirmed and goto step 2.} \end{cases}$$

- Step 2: Check the battery charging status as -

$$C_{BESS} > 80\% \begin{cases} Yes & \text{Then charging off and disconnect battery and goto step 3.} \\ No & \text{Then goto step 3.} \end{cases}$$

- Step 3: Check the different frequency active power differences between source-load pairs at MF bus ($P_{b-f-var}$), calculate the reference current for grid side converter and battery and goto step 10.

$$I_G^* = \frac{\sum_{f=1}^{n} P_{b-f-var}}{v_{b-50}},\ I_{BESS}^* = \frac{P_{BESS}}{v_{b-0}}$$

- Step 4: Check the different frequency active power differences between source-load pairs at MF bus and find out the availability of battery power as-

$$P_{ESS} > P_{BESS-max} \begin{cases} Yes & \text{Then load shedding and goto step 4.} \\ No & \text{Then goto step 5.} \end{cases}$$

- Step 5: Check charging or discharging mode of battery as-

$$P_{BESS} > 0 \begin{cases} Yes & \text{Battery acts as load, in charging mode and goto step 6.} \\ No & \text{Battery acts as source, in discharging mode and goto step 9.} \end{cases}$$

- Step 6: Check the battery charging status as -

$$C_{BESS} > 80\% \begin{cases} Yes & \text{Then charging off and disconnect battery and go for source side control and goto step 5.} \\ No & \text{Then goto step 7.} \end{cases}$$

- Step 7: Check the different frequency active power differences between source-load pairs and battery at MF bus and goto step 8.

$$P_{b-f-var} = P_{b-f-L} - P_{b-f-S} + \frac{P_{BESS}}{n}$$

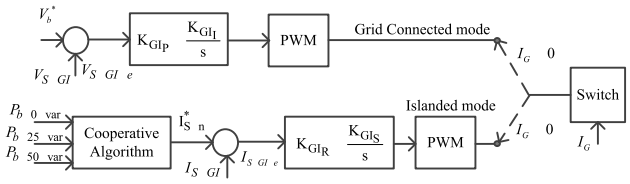

FIGURE 5. Control strategy of grid interactive converter in grid connected and islanded modes.

- Step 8: Check -

$$P_{b-f-var} > 0 \begin{cases} Yes & \text{This frequency source is at max available value but can't fulfill the paired load demand, so operated at max available power and that paired load takes excess power from other frequency sources equally, goto step 10.} \\ & I_{s-j}^* = I_{s-j-av} \\ No & \text{This frequency source fulfill the paired load demand by not reaching max avaiable power, so it supply power to other frequency loads and battery then goto step 10.} \\ & I_{s-k}^* = I_{l-k} + \frac{\sum_{f=1}^{n} P_{b-f-var}}{n-x} + \frac{I_{BESS}}{n-x} \end{cases}$$

- Step 9: Check the battery discharging status as -

$$C_{BESS} < 20\% \begin{cases} Yes & \text{Then discharging off and disconnect battery and go for load shedding and goto step 5.} \\ No & \text{Then goto step 7.} \end{cases}$$

- Step 10: Check for source and load power fluctuation -

$$P_{b-f-S-var}/P_{b-f-L-var} = 0 \begin{cases} Yes & \text{Total active power is balanced.} \\ No & \text{Goto step 1.} \end{cases}$$

B. CONTROL STRATEGY FOR GRID INTERACTIVE CONVERTER

The control strategy for grid side [39], grid forming [39], grid feeding [39], and load side converter [4], [10] are already explained. The grid interactive (GI) converter is a special converter that acts as a grid feeding converter to supply active power in grid connected mode and acts as a grid forming converter to balance the MF bus voltage in islanded mode. The control strategy of the GI converter is shown in Fig. 5.

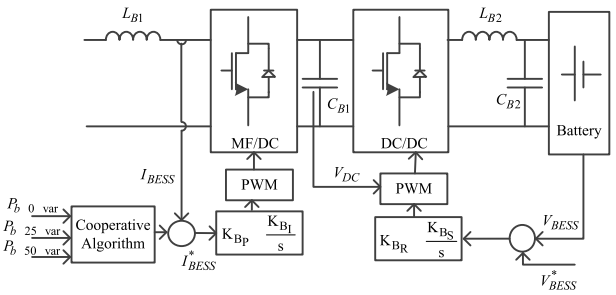

FIGURE 6. Control strategy of BESS.

According to the cooperative algorithm the output reference current (I^*_{S-n}) of the GI converter is calculated in grid connected mode. To control the output current of the DC/MF GI converter, the inner current loop of the average current control method is applied. The current difference (I_{S-GI-e}) is passed through a designed PI controller. The output of the controller is sent to the pulse width modulation (PWM) block to generate the switching signal. Here PWM control is used as it has lower switching loss. In islanded mode, as the grid becomes absent, the grid interactive converter behaves like a grid forming converter and supports MF bus voltage. Here, the output voltage (V_{S-GI}) of the DC/MF converter is sensed and compared with the reference MF bus voltage (V^*_b). The voltage error (V_{S-GI-e}) is given to a designed PI controller to produce the modulating signal for PWM voltage control.

C. CONTROL STRATEGY FOR BESS

In MFMG, the BESS is connected by a back to back converter structure to control the active power flow of the battery. The control structure of BESS is presented in Fig. 6. The DC/MF converter controls the output current of BESS. Here average current control method is applied and accordingly PI controller design is performed. Here, the reference output current (I^*_{BESS}) is calculated from the cooperative control algorithm. The actual output current (I_{BESS}) is sensed and compared with the reference current. The current error (I_{BESS-e}) is passed through the PI controller to generate the modulating signal. A bidirectional buck-boost converter is adopted to control the battery voltage. The voltage mode control strategy is applied and suitable PI parameters are chosen for the controller.

D. PI CONTROLLER DESIGN

First the modelling of DC/MF converter is executed. The two operation modes of DC/MF converter is shown in Fig. 7. By using inductor volt-sec balance and capacitor charge balance criteria, state space equations for each mode are derived. Here all switches are considered ideal and the ESR of the inductor is neglected. Next the small signal model of DC/MF converter is formed and the required transfer function (TF) is calculated for controller design.

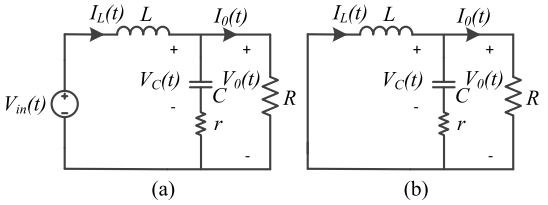

FIGURE 7. (a) Equivalent circuit of converter in DT_S mode (b) Equivalent circuit of converter in $(1-D)T_S$ mode.

TABLE 3. Controller parameters for different converters of MFMG.

Converter name	Proportional Gain (K_P)	Integral Gain (K_I) in S^{-1}
Grid side	$K_{G_P} = 1.8, K_{G_R} = 3.6$	$K_{G_I} = 78.4, K_{G_S} = 62.6$
Grid forming	$K_{GF_P} = 1.2$	$K_{GF_I} = 45$
Grid feeding	$K_{GFE_P} = 18.7$	$K_{GFE_I} = 345$
Grid interactive	$K_{GI_P} = 5, K_{GI_R} = 1.5$	$K_{GI_I} = 120.5, K_{GI_S} = 25$
BESS	$K_{B_P} = 18.3, K_{B_R} = 7.8$	$K_{B_I} = 165, K_{B_S} = 75$

The output voltage to input voltage TF of the converter is defined as,

$$\frac{\hat{V}_0(S)}{\hat{V}_{in}(S)} = \frac{RD(1+SrC)/(R+r)LC}{S^2LC(R+r)+S(L+rRC)+R} \tag{8}$$

In this paper, a PI controller is designed for voltage mode control. So output voltage (V_0) to duty cycle (d) TF needs to be obtained.

$$\frac{\hat{V}_0(S)}{\hat{d}(S)} = \frac{RV_{in}(1+SrC)/(R+r)LC}{S^2LC(R+r)+S(L+rRC)+R} \tag{9}$$

For average mode current control, the inductor current (I_L) to duty cycle (d) TF needs to be obtained.

$$\frac{\hat{I}_L(S)}{\hat{d}(S)} = \frac{V_{in}(1+SC(r+R))/(R+r)LC}{S^2LC(R+r)+S(L+rRC)+R} \tag{10}$$

Here loop shaping method is used for the PI controller designs of voltage mode and average current mode control. The objective of the controller design is to maintain a decent phase margin at the gain crossover frequency (GCF) to make the total close loop system stable. The GCF of voltage and current loop are chosen as 4 kHz and 30 kHz respectively based on the switching frequency (100 kHz). Different PI controllers for grid side, grid forming, grid feeding, grid interactive, and BESS side converter are designed and the PI parameters are presented in Table 3.

V. SIMULATION RESULT

A 9 bus MFMG with ESS as shown in Fig. 3 is simulated in islanded and grid connected mode. All filters are designed based on the assumption that a maximum of 10% ripple is allowed in the capacitor voltages and 5% ripple is allowed for inductor currents. The filter parameters are presented in Table 6. Different active power imbalance cases are created during different operation scenarios of MFMG. The simulation results for all those cases are presented in this section and effectiveness of the algorithm is evaluated with proper analysis of each case.

TABLE 4. Case study of 9 bus MFMG.

Source/ Load	Operating frequency	Voltage	Maximum capacity	Type of converter connected	Bus No.
Grid	50 Hz	230 V	-	AC50/DC, DC/MF	2
PV	DC	300 V	100 kW	DC/DC, DC/MF	3
WT	25 Hz	150 V	80 kW	AC25/DC, DC/MF	4
MT	50 Hz	230 V	60 kW	AC50/DC, DC/MF	5
EV	DC	110 V	60 kW	MF/DC, DC/DC	6
DL	25 Hz	230 V	70 kW	MF/DC, DC/AC25	7
IL	50 Hz	230 V	80 kW	MF/DC, DC/AC50	8
BESS	DC	475 V	50 kW	MF/DC, DC/DC	9

V_{MFB}: 500 V DC + 100 V AC 25 Hz (RMS) + 230 V AC 50 Hz (RMS)

TABLE 5. Simulation parameters of MFMG.

Parameter	value
L_{G-F}, C_{G-F}	$1.5mH, 750\mu F$
L_{GF-F}, C_{GF-F}	$1mH, 1000\mu F$
L_{GFE-F}	$1mH$
L_{L-F}, C_{L-F}	$0.2mH, 400\mu F$
L_{BESS-F}, C_{BESS-F}	$0.5mH, 600\mu F$
$C_{G-B}, C_{GF-B}, C_{GFE-B}, C_{BESS-B}$	$1000\mu F$
$C_{BL-0}, C_{BL-50}, C_{BL-25}$	$1000\mu F$

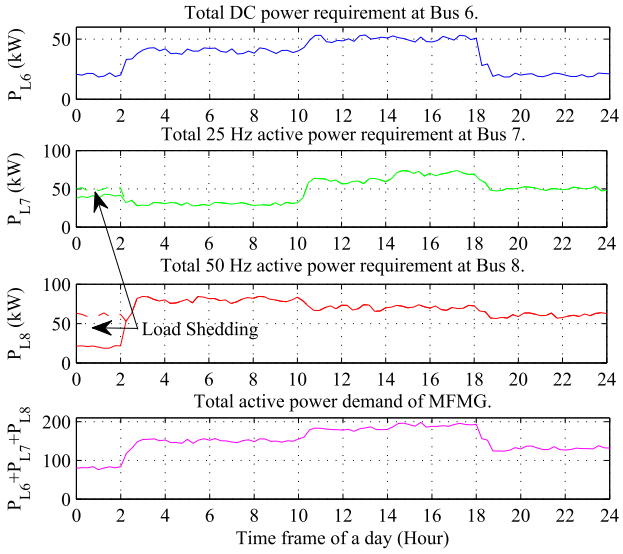

FIGURE 8. Total DC (P_{L6}), 25 Hz (P_{L7}) and 50 Hz (P_{L8}) active power requirement in bus 6, 7, and 8.

A. ISLANDED MODE

In this mode, total load of MFMG should be supplied by the sources and the battery as the grid is disconnected. Different frequency loads prefer to take active power from their paired source. If still more power is required then they take powers from all other available sources and battery. As the loads are variable so different active power imbalance cases are created during different time of a day. All the sources and battery need to be controlled properly to balance different frequency active powers in those cases.

An electric vehicle (EV) charging station (DC), domestic load (25 Hz), and industrial load (50 Hz) are connected to buses 6, 7, and 8 respectively where the EV load is a sensitive load. These three load profiles are presented in Fig. 8. It can

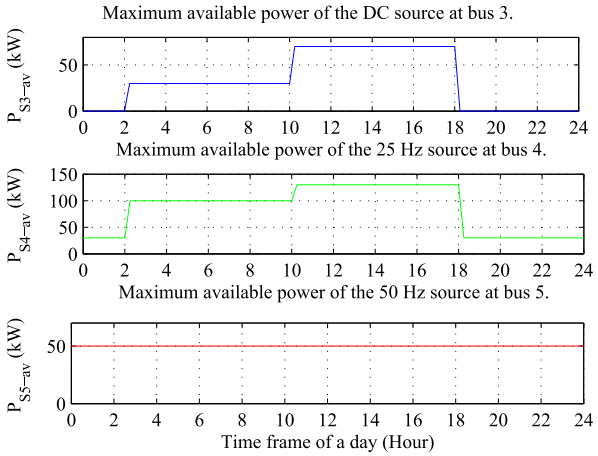

FIGURE 9. Maximum available DC (P_{S3-av}), 25 Hz (P_{S4-av}) and 50 Hz (P_{S5-av}) active power in bus 3, 4, and 5.

be noticed that all the loads vary as per their nature throughout the day. At 00:00, the SOC of the battery reaches 20% so the battery got disconnected. In 00:00 to 02:00, total load (140 kW) becomes higher than total source (80 kW). In this situation, some portions of the industrial and domestic load are shredded. Industrial load is decreased from 60 kW to 20 kW and domestic load is decreased from 50 kW to 40 kW. For all other times of the day, the MFMG is able to deliver the total load power.

A PV source (DC), two WT sources (25 Hz), and one MT unit (50 Hz) are connected in buses 3, 4, and 5 respectively. In islanded mode, one of the wind turbines is working as grid interactive source and balances the MF bus (bus 1) voltage. Fig. 9 represents the availability of the sources throughout the day. The MT unit is available throughout the day. The PV source is only available in the daytime and creates the maximum amount of active power between 10:00 to 18:00. The availability of WT source depends upon the wind speed and it generates variable active power throughout the day.

To meet the variable load demands of MFMG, the sources need to be properly controlled. Here, the source side control is implemented based on the proposed cooperative algorithm. Four different active power imbalance cases are investigated to verify the algorithm in the islanded mode of operation of MFMG. The source side converters can create any other required frequency active power from the source power. Source power at bus 3 (DC), bus 4 (25 Hz), and bus 5 (50 Hz) are presented in Fig. 10, Fig. 11, and Fig. 12 respectively for different time of a day. It can be seen that between 02:00 to 10:00, the active power difference among different source-load pairs are $P_{b-0-diff} > 0$, $P_{b-25-diff} = 0$, and $P_{b-50-diff} > 0$, which is the condition for case 5. For this case, only the active power of the 25 Hz source-load pair is balanced but the DC and 50 Hz source can't fulfill their paired load demand. So the DC (L_6) and 50 Hz load (L_8) take the required 10 kW DC and 30 kW 50 Hz active power from 25 Hz source (S_4). For this condition, the battery

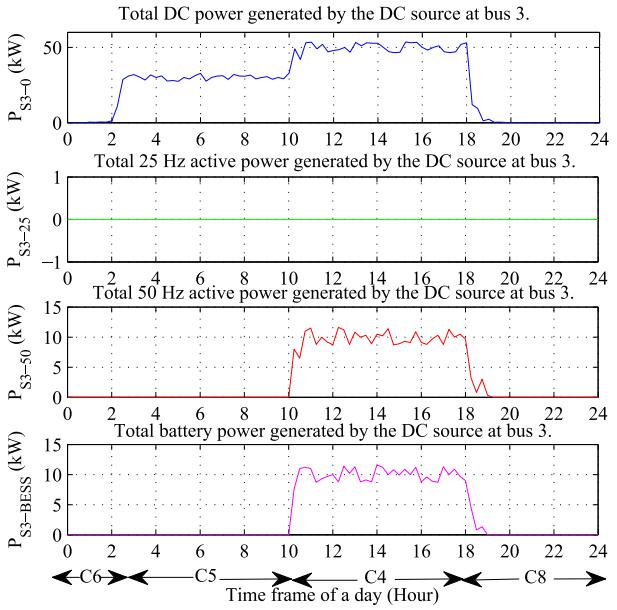

FIGURE 10. Total DC power is converted to DC (P_{S3-0}), 25 Hz (P_{S3-25}), 50 Hz (P_{S3-50}), and battery power ($P_{S3-BESS}$) by DC source (bus 3) converter and sent to MF bus.

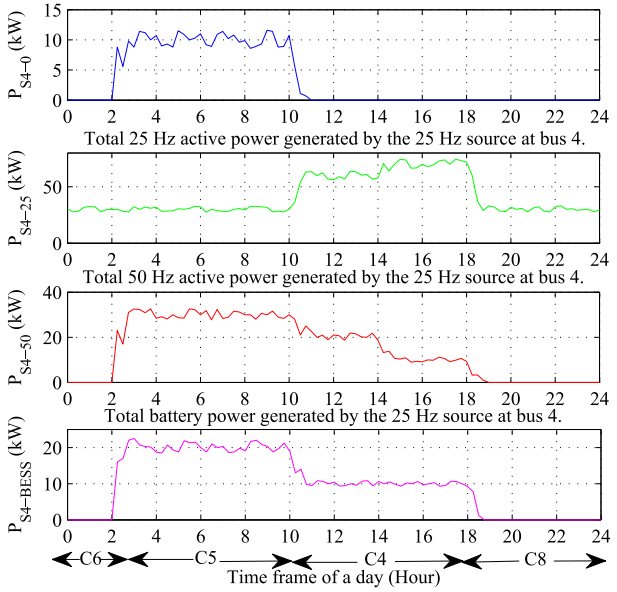

FIGURE 11. Total 25 Hz active power is converted to DC (P_{S4-0}), 25 Hz (P_{S4-25}), 50 Hz (P_{S4-50}), and battery power ($P_{S4-BESS}$) by 25 Hz source (bus 4) converter and sent to MF bus.

is at charging mode and takes the required 20 kW active power from 25 Hz source (S_4). Between 10:00 to 18:00, the active power difference between different source-load pairs are, $P_{b-0-diff} = 0$, $P_{b-25-diff} = 0$, and $P_{b-50-diff} > 0$ (case 4). Here the active power of DC and 25 Hz source-load pairs are balanced but 50 Hz source-load pair active power is not balanced. So here, the 50 Hz load (L_8) takes equally 10 kw 50 Hz active power from the DC (S_3) and 25 Hz source (S_4). The battery is at charging mode and takes 10 kW

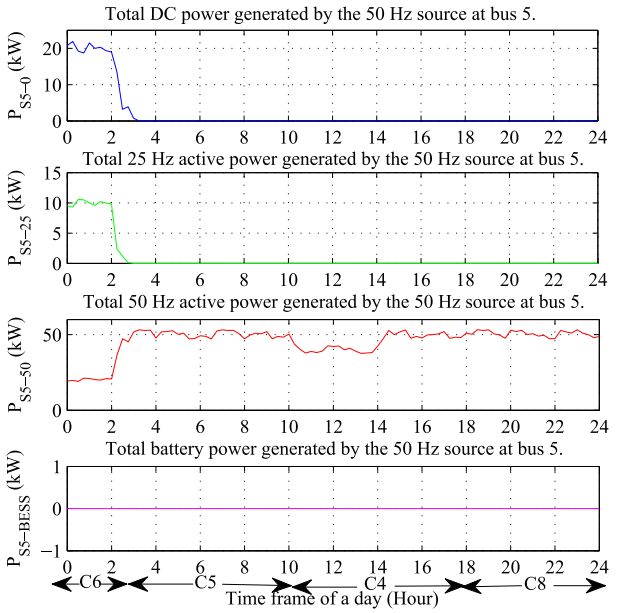

FIGURE 12. Total 50 Hz active power is converted to DC (P_{S5-0}), 25 Hz (P_{S5-25}), 50 Hz (P_{S5-50}), and battery power ($P_{S5-BESS}$) by 50 Hz source (bus 5) converter and sent to MF bus.

equally from the DC (S_3) and 25 Hz source (S_4). Between 18:00 to 24:00, the active power difference among different source-load pairs are $P_{b-0-diff} > 0$, $P_{b-25-diff} > 0$, and $P_{b-50-diff} > 0$, so case 8 happens. In this case, all sources are at their maximum available limit but can't fulfill their paired load active power demand. In this condition, the DC load (L_6) takes 20 kW DC power from the battery, 25 Hz load (L_7) takes 20 kW 25 Hz power from the battery and the 50 Hz load (L_8) takes 10 kW 50 Hz power from the battery. The battery is at discharging mode and sends 50 kW active power to the MF bus (bus 1) for active power balancing. At 24:00, the SOC level of the battery reaches 20%, so it is disconnected from the MFMG. In this situation some portion of the 25 Hz (L_7) and 50 Hz load (L_8) are shredded and the active power difference among different source load pair becomes $P_{b-0-diff} > 0$, $P_{b-25-diff} > 0$, and $P_{b-50-diff} = 0$ (case 6). For this case, the active power demand of 50 Hz load (L_8) is fulfilled but DC and 25 Hz active powers are not balanced. Here DC (L_6) and 25 Hz load (L_7) take 20 kW DC power and 10 kW 25 Hz power from 50 Hz source (S_5). All source and load powers of MFMG are presented in Table 6.

The BESS is either in charging mode or in discharging mode based on the operating scenarios. If total source power of the MFMG is higher than load power ($\sum_{f=1}^{n} P_{b-f-S} - \sum_{f=1}^{n} P_{b-f-L} > 0$) then BESS is charged. If total load power is higher ($\sum_{f=1}^{n} P_{b-f-S} - \sum_{f=1}^{n} P_{b-f-L} < 0$) then BESS is discharged and provides the required active power for power balancing. So for case 8, the BESS should discharge and for all other cases, BESS should charge. In Fig. 13, the total battery power ($P_{BESS} = P_{BESS-0} + P_{BESS-25} + P_{BESS-50}$) is provided where total battery power is converted to different frequency active powers by the BESS side DC/MF converter

TABLE 6. Different source and load powers of MFMG in Islanded condition.

Time	P_{s3}	P_{s4}	P_{s5}	P_{sT}	P_{l6}	P_{l7}	P_{l8}	P_{lT}	P_9
0-2	0	30	50	80	20	40	20	80	0
2-4	30	90	50	170	40	30	80	150	-20
4-6	30	90	50	170	40	30	80	150	-20
6-8	30	90	50	170	40	30	80	150	-20
8-10	30	90	50	170	40	30	80	150	-20
10-12	70	90	40	200	50	60	70	180	-20
12-14	70	90	40	200	50	60	70	180	-20
14-16	70	90	50	210	50	70	70	190	-20
16-18	70	90	50	210	50	70	70	190	-20
18-20	0	30	50	80	20	50	60	130	50
20-22	0	30	50	80	20	50	60	130	50
22-24	0	30	50	80	20	50	60	130	50

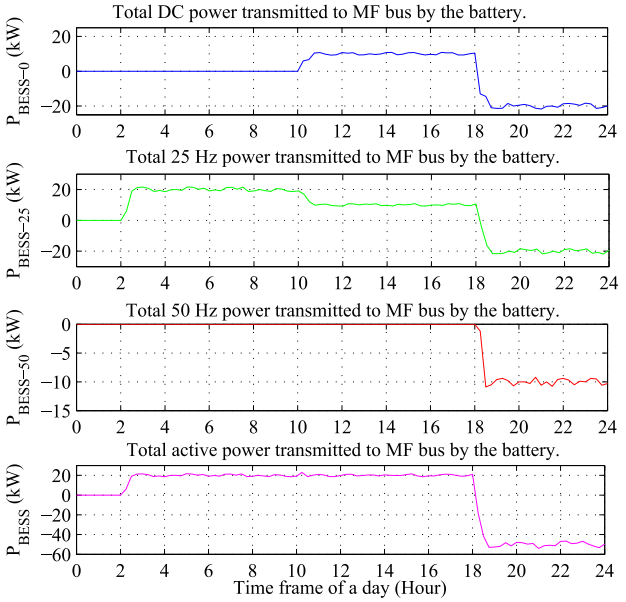

FIGURE 13. Total active power exchange of the battery with MF bus which contains three different frequencies ($P_{BESS} = P_{BESS-0} + P_{BESS-25} + P_{BESS-50}$).

and sent to the MF bus (bus 1). It can be noticed that between 02:00 to 18:00, the battery is getting charged by taking 20 kW power from the available sources. In between 18:00-24:00, case 8 happens and BESS provides 50 kW active power to the MF bus to create the active power balance condition. At 22:00, the SOC level of the battery becomes 20% and it is disconnected from the MFMG system.

The total active power of the sources at bus 3 ($P_{S3} = P_{S3-0} + P_{S3-25} + P_{S3-50} + P_{S3-BESS}$), 4, and 5 is presented in Fig. 14. Total source power of the MFMG is calculated by adding the S_3, S_4, and S_5 active powers. It can be noticed from the result that the algorithm maintains the active power balancing condition for islanded mode($P_{BESS} = (P_{S3}+P_{S4}+P_{S5})$- $(P_{L6}+P_{L7}+P_{L8})$. So the proposed algorithm is working precisely for islanded mode of operation of MFMG.

To verify the active power balance conditions, different frequency incoming source active powers are measured and compared with different frequency outgoing load active powers at MF bus (bus 1). Total DC ($P_{b-0-S} = P_{S3-0} + P_{S4-0} + P_{S5-0} + P_{S3-BESS}$), 25 Hz and 50 Hz power, which are generated by different sources and received at MF bus is

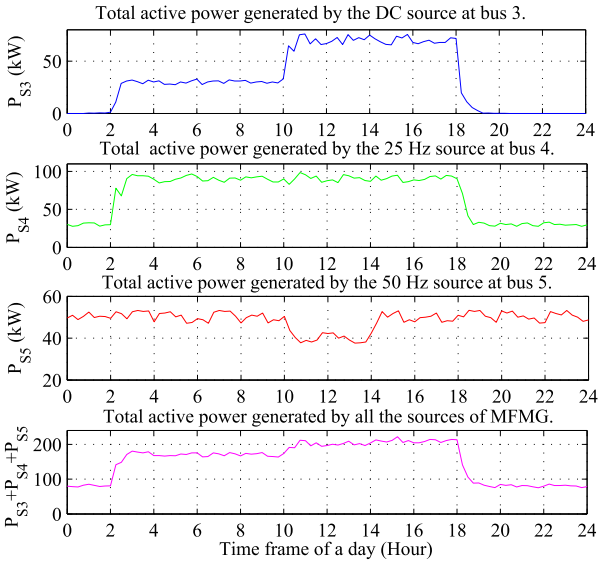

FIGURE 14. Total active power generation of the sources at bus 3 (P_{S3}), bus 4 (P_{S4}) and bus 5 (P_{S5}) of the MFMG.

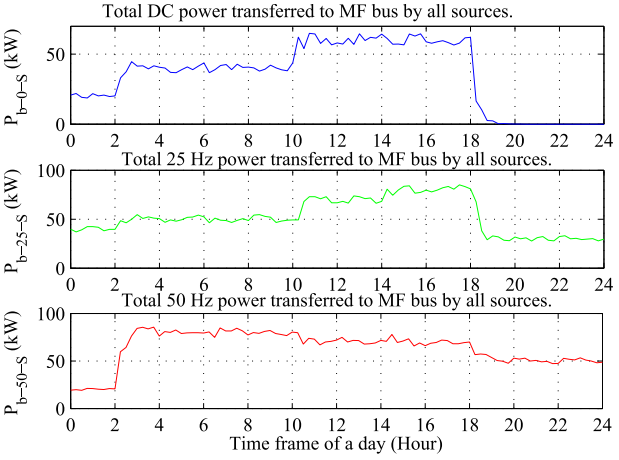

FIGURE 15. Total DC (P_{b-0-S}), 25 Hz (P_{b-25-S}), and 50 Hz (P_{b-50-S}) active powers received at MF bus (bus 1) from different sources of MFMG.

shown in Fig. 15. It can be seen from the result that every incoming frequency active power matches with that frequency load power at MF bus. So, $P_{b-0-S} = P_{L6} + P_{BESS-0}$, $P_{b-25-S} = P_{L7} + P_{BESS-25}$, $P_{b-50-S} = P_{L8} + P_{BESS-50}$ and $P_{S3} \neq P_{L6}$, $P_{S4} \neq P_{L7}$, $P_{S5} \neq P_{L8}$. So it can be concluded from the results that if the MFMG maintains the active power balance condition, then different frequency active powers get balanced at the MF bus, so the conditions are well defined.

B. GRID CONNECTED MODE

Here, the MFMG is simulated in grid connected mode and the algorithm is verified. The grid should supply the active power differences between different frequency source-load pairs and the battery power. For the simulation purpose, the total grid connected time cycle has been chosen as 24 hours. The grid interactive converter works as a grid feeding converter. So, the available active power at bus 4 doubles as both WTs are

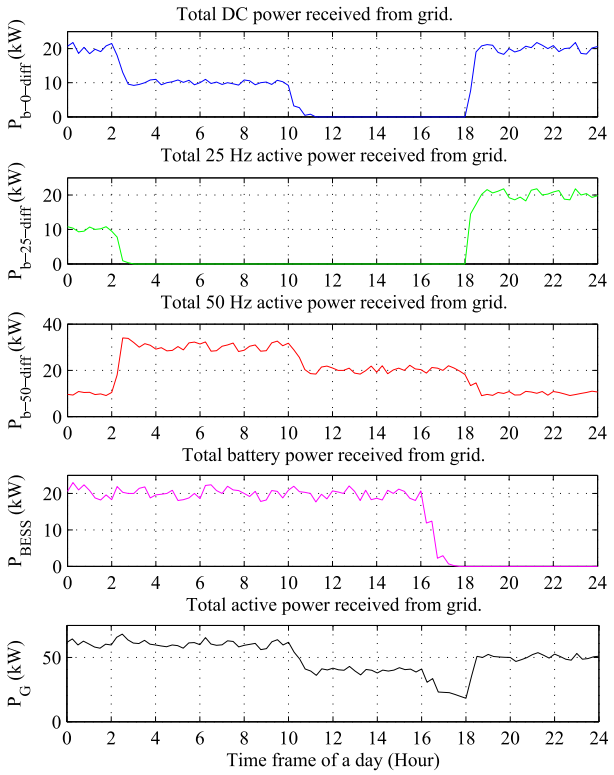

FIGURE 16. Output power of the grid side converter (P_G) which is converted to different frequency active powers ($P_G = P_{b-0-diff} + P_{b-25-diff} + P_{b-50-diff} + P_{BESS}$) and transmitted to bus 1.

available for sending power to the MF bus (bus 1). In grid connected mode the domestic load is also increased as grid power is cheaper than battery power. In this mode, the BESS is only charged and is disconnected from MFMG when the SOC level climbs 80%.

Simulation result with the different operating conditions for grid connected mode is conferred in Fig. 16. Between 00:00-02:00, $P_{b-0-diff} = 20\ kW$, $P_{b-25-diff} = 10\ kW$, $P_{b-50-diff} = 10\ kW$, and $P_{BESS} = 20\ kW$. So grid delivers a total of 60 kW active power, which is converted to different frequency active powers by grid side DC/MF converter and sends that to MF bus. Similarly, between 10:00-16:00, the grid generates 40 kW active power to balance the power imbalance situation of MFMG. At 16:00, the SOC level of the battery reaches 80% and the battery is disconnected. From 18:00 to 24:00, the grid sends a total of 50 kW active power, which is converted to 20 kW DC + 20 kW 25 Hz + 10 kW 50 Hz active powers. Here as per the proposed algorithm active power balancing condition of MFMG in grid connected mode ($P_G = \sum_{f=1}^{n} P_{b-f-diff} + P_{BESS}$) is maintained and grid can balance different active power imbalance scenarios of MFMG. So, the algorithm works flawlessly in grid connected mode. The performance comparison of the proposed controller with other related work existing in the literature i.e. [15], [32] is shown in Table 7. It can be noticed that multifrequency operation is not possible with other control strategies and the proposed controller drastically

TABLE 7. Performance comparison of proposed controller with existing literature.

References	[15], [32].	This work.
Topology	Droop control.	Traditional P-Q control.
Modulating signal for PWM	DC or AC.	Multifrequency.
Multifrequency operation	Not possible.	possible.
Power imbalance cases solved	Maximum four cases.	Eight cases.
Rise Time of V_{b-f-S}	$0.022sec$	$0.036sec$
Rise Time of P_{b-f-S}	$0.015sec$	$0.018sec$
Peak overshoot of V_{b-f-S}	12.5%	0.8%
Peak overshoot of P_{b-f-S}	12%	0.6%
Steady state error of V_{b-f-S}	1.5%	0.2%
Steady state error of P_{b-f-S}	5%	0.2%

improved the peak overshoot and steady-state error response of the system.

VI. CONCLUSION

In MFMG, different frequency powers are superimposed on the MF bus and the consumers have a special ability to choose among the available powers alternatively at different time frames. This frequency selective power consumption creates variable active power demands at the load side and several new active power imbalance situations develop. In this paper, a new power management structure of MFMG is introduced where several source-load pairs are operated at different frequencies based on their distance. A cooperative control algorithm is proposed for the sources and battery to get the active power balance of the different source-load pairs. The performance evaluation of MFMG with the proposed algorithm for generation control of the sources and the control strategy of BESS has been examined under different operating scenarios in grid connected and islanded modes. Several active power unbalance case studies have been conducted to present the effectiveness of the algorithm in Matlab Simulink.

In islanded mode, it can be noticed that for each active power imbalance case, the ESS is controlled in such a way that total active power gets balanced between different frequency sources and loads ($P_{BESS} = P_{ST} - P_{LT}$). In this condition, each frequency incoming active power at MF bus matches with that frequency load power ($P_{b-0-f} = P_{L-f} - P_{BESS-f}$). According to the algorithm, the ESS takes 20 kW power between 02:00-18:00 and gives 60 kW power between 18:00-24:00 to maintain the active power balance in islanded mode. At 24:00, the SOC level of the battery becomes 20% and the battery gets disconnected from the MFMG between 00:00-02:00 and load shedding is done. In grid connected mode it can be noticed that the grid maintains the active power balance of MFMG by providing the required active powers ($(P_G = \sum_{f=1}^{n} P_{b-f-diff} + P_{BESS})$). The grid sends 60 kW in between 00:00-10:00, 40 kW in between 10:00-16:00, 20 kW in between 16:00-18:00, and 50 kW in between 18:00-24:00 as per the algorithm and maintains the active power balance. In grid connected mode the ESS is charged between 00:00-16:00 and gets disconnected from the MFMG as the SOC level reaches 80%. It can be concluded from the results that the sources and BESS behave exactly as per the algorithm rules. So the controllers are perfectly designed. The results also indicate that the proposed algorithm balances the active

power of the MFMG system for all eight power imbalance cases. So the algorithm is properly drafted for grid connected and islanded modes.

The work presented in this paper mainly focuses on the active power balancing problem of MFMG with ESS based on source-load pair distance. Different new power balancing algorithms of MFMG can be proposed in the future based on the cost, reliability, or availability of the sources. The basic concept of the paper can be applied to a cluster of microgrids where some microgrids act as sources and other microgrids act as loads. Sensitivity analysis of MFMG is another important aspect that can be explored in the future.

REFERENCES

[1] M. Rezkallah, A. Chandra, B. Singh, and S. Singh, "Microgrid: Configurations, control and applications," *IEEE Trans. Smart Grid*, vol. 10, no. 2, pp. 1290–1302, Mar. 2019.

[2] M. Ganjian-Aboukheili, M. Shahabi, Q. Shafiee, and J. M. Guerrero, "Seamless transition of microgrids operation from grid-connected to islanded mode," *IEEE Trans. Smart Grid*, vol. 11, no. 3, pp. 2106–2114, May 2020.

[3] M. Faisal, M. A. Hannan, P. J. Ker, A. Hussain, M. B. Mansor, and F. Blaabjerg, "Review of energy storage system technologies in microgrid applications: Issues and challenges," *IEEE Access*, vol. 6, pp. 35143–35164, 2018.

[4] R. Dey and S. Nath, "Architecture and power converter for multifrequency microgrid," in *Proc. Nat. Power Electron. Conf. (NPEC)*, Dec. 2019, pp. 1–6.

[5] J. A. Ferreira, "Nestled secondary power loops in multilevel modular converters," in *Proc. IEEE 15th Workshop Control Modeling Power Electron. (COMPEL)*, Jun. 2014, pp. 1–9.

[6] R. Dey and S. Nath, "A new power distribution concept for multifrequency microgrid," in *Proc. IEEE 12th Energy Convers. Congr. Expo. Asia (ECCE–Asia)*, May 2021, pp. 491–496.

[7] S. Brüske, G. De Carne, and M. Liserre, "Multi-frequency power transfer in a smart transformer based distribution grid," in *Proc. IECON 40th Annu. Conf. IEEE Ind. Electron. Soc.*, Oct. 2014, pp. 4325–4331.

[8] S. Akshatha, C. N. Arun, V. S. Abhijith, and B. G. Fernandes, "A unified AC-DC microgrid architecture for distribution of AC and DC power on the same line," in *Proc. IEEE Appl. Power Electron. Conf. Expo. (APEC)*, Mar. 2017, pp. 430–433.

[9] K. Terada, "Application and economical evaluation of the superposed AC and DC power transmission system," *Electr. Eng. Jpn.*, vol. 98, no. 1, pp. 114–120, 1978.

[10] M. Gagic, I. Pecelj, Z. Qin, and J. Ferreira, "Control of load interfacing power electronics converter in multifrequency systems," in *proc. IEEE 10th Int. Conf. Power Electron. ECCE Asia (ICPE-ECCE Asia)*, May 2019, pp. 1574–1580.

[11] A. Conde, G. Perez, G. Gutierrez-Alcaraz, and Z. Leonowicz, "Frequency improvement in microgrids through battery management system control supported by a remedial action scheme," *IEEE Access*, vol. 10, pp. 8081–8091, 2022.

[12] S. Gangatharan, M. Rengasamy, R. M. Elavarasan, N. Das, E. Hossain, and V. M. Sundaram, "A novel battery supported energy management system for the effective handling of feeble power in hybrid microgrid environment," *IEEE Access*, vol. 8, pp. 217391–217415, 2020.

[13] T. Zhao and Z. Ding, "Cooperative optimal control of battery energy storage system under wind uncertainties in a microgrid," *IEEE Trans. Power Syst.*, vol. 33, no. 2, pp. 2292–2300, Mar. 2018.

[14] M. Kumar, S. C. Srivastava, and S. N. Singh, "Control strategies of a DC microgrid for grid connected and islanded operations," *IEEE Trans. Smart Grid*, vol. 6, no. 4, pp. 1588–1601, Jul. 2015.

[15] P. C. Loh, D. Li, Y. K. Chai, and F. Blaabjerg, "Autonomous control of interlinking converter with energy storage in hybrid AC–DC microgrid," *IEEE Trans. Ind. Appl.*, vol. 49, no. 3, pp. 1374–1382, May 2013.

[16] M. M. Ismail, A. F. Bendary, and M. Elsisi, "Optimal design of battery charge management controller for hybrid system pv/wind cell with storage battery," *Int. J. Power Energy Convers.*, vol. 11, no. 4, pp. 412–429, 2020.

[17] Z. Yuan, S. W. H. de Haan, J. B. Ferreira, and D. Cvoric, "A FACTS device: Distributed power-flow controller (DPFC)," *IEEE Trans. Power Electron.*, vol. 25, no. 10, pp. 2564–2572, Oct. 2010.

[18] V. Chitransh, A. Shetty, A. K. Das, J. O. Ojo, M. Veerachary, B. G. Fernandes, and J. A. Ferreira, "Evaluation of multifrequency power electronic converters: Concept, architectures, and realization," *IEEE J. Emerg. Sel. Topics Power Electron.*, vol. 9, no. 3, pp. 3582–3597, Jun. 2021.

[19] S. Ganesan, U. Subramaniam, A. A. Ghodke, R. M. Elavarasan, K. Raju, and M. S. Bhaskar, "Investigation on sizing of voltage source for a battery energy storage system in microgrid with renewable energy sources," *IEEE Access*, vol. 8, pp. 188861–188874, 2020.

[20] M. S. Mahdavi, G. B. Gharehpetian, and H. A. Moghaddam, "Enhanced frequency control method for microgrid-connected flywheel energy storage system," *IEEE Syst. J.*, vol. 15, no. 3, pp. 4503–4513, Sep. 2021.

[21] L. Chen, H. Chen, Y. Li, G. Li, J. Yang, X. Liu, Y. Xu, L. Ren, and Y. Tang, "SMES-battery energy storage system for the stabilization of a photovoltaic-based microgrid," *IEEE Trans. Appl. Supercond.*, vol. 28, no. 4, pp. 1–7, Jun. 2018.

[22] Z. Yang, L. Xia, and X. Guan, "Fluctuation reduction of wind power and sizing of battery energy storage systems in microgrids," *IEEE Trans. Autom. Sci. Eng.*, vol. 17, no. 3, pp. 1195–1207, Jul. 2020.

[23] H. Xie, X. Teng, Y. Xu, and Y. Wang, "Optimal energy storage sizing for networked microgrids considering reliability and resilience," *IEEE Access*, vol. 7, pp. 86336–86348, 2019.

[24] R. Ahshan, S. A. Saleh, and A. Al-Badi, "Performance analysis of a dq power flow-based energy storage control system for microgrid applications," *IEEE Access*, vol. 8, pp. 178706–178721, 2020.

[25] X. Zheng, Q. Li, P. Li, and D. Ding, "Cooperative optimal control strategy for microgrid under grid-connected and islanded modes," *Int. J. Photoenergy*, vol. 2014, pp. 1–11, May 2014.

[26] M. H. Moradi, M. Eskandari, and S. M. Hosseinian, "Cooperative control strategy of energy storage systems and micro sources for stabilizing microgrids in different operation modes," *Int. J. Elect. Power Energy Syst.*, vol. 78, pp. 390–400, Jun. 2016.

[27] D. Papadaskalopoulos, D. Pudjianto, and G. Strbac, "Decentralized coordination of microgrids with flexible demand and energy storage," *IEEE Trans. Sustain. Energy*, vol. 5, no. 4, pp. 1406–1414, Oct. 2014.

[28] A. K. Barik and D. C. Das, "Active power management of isolated renewable microgrid generating power from rooftop solar arrays, sewage waters and solid urban wastes of a smart city using salp swarm algorithm," in *Proc. Technol. Smart-City Energy Secur. Power (ICSESP)*, Mar. 2018, pp. 1–6.

[29] M. Elsisi, "New design of robust PID controller based on meta-heuristic algorithms for wind energy conversion system," *Wind Energy*, vol. 23, no. 2, pp. 391–403, Feb. 2020.

[30] M. Elsisi, M. Soliman, M. Aboelela, and W. Mansour, "GSA-based design of dual proportional integral load frequency controllers for nonlinear hydrothermal power system," *World Academy Sci., Eng. Technol.*, vol. 9, pp. 1142–1148, Aug. 2015.

[31] M. Faisal, M. A. Hannan, P. J. Ker, and M. N. Uddin, "Backtracking search algorithm based fuzzy charging-discharging controller for battery storage system in microgrid applications," *IEEE Access*, vol. 7, pp. 159357–159368, 2019.

[32] X. Lu, K. Sun, J. M. Guerrero, J. C. Vasquez, and L. Huang, "State-of-charge balance using adaptive droop control for distributed energy storage systems in DC microgrid applications," *IEEE Trans. Ind. Electron.*, vol. 61, no. 6, pp. 2804–2815, Jun. 2014.

[33] J. M. Guerrero, P. C. Loh, T.-L. Lee, and M. Chandorkar, "Advanced control architectures for intelligent microgrids—Part II: Power quality, energy storage, and AC/DC microgrids," *IEEE Trans. Ind. Electron.*, vol. 60, no. 4, pp. 1263–1270, Apr. 2013.

[34] L. Yang and Z. Hu, "Coordination of generators and energy storage to smooth power fluctuations for multi-area microgrid clusters: A robust decentralized approach," *IEEE Access*, vol. 9, pp. 12506–12520, 2021.

[35] J. Lai, X. Lu, X. Yu, and A. Monti, "Cluster-oriented distributed cooperative control for multiple AC microgrids," *IEEE Trans. Ind. Informat.*, vol. 15, no. 11, pp. 5906–5918, Nov. 2019.

[36] R. M. Kamel and B. Kermanshahi, "Design and implementation of models for analyzing the dynamic performance of distributed generators in the micro grid—Part I: Micro turbine and solid oxide fuel cell," Dept. Elect. Eng., Tokai Univ., Tokyo, Japan, Tech. Rep., 2010.
[37] C. Renno and F. Petito, "Design and modeling of a concentrating photovoltaic thermal (CPV/T) system for a domestic application," *Energy Buildings*, vol. 62, pp. 392–402, Jul. 2013.
[38] A. K. Saha, S. Chowdhury, S. P. Chowdhury, and P. A. Crossley, "Modeling and performance analysis of a microturbine as a distributed energy resource," *IEEE Trans. Energy Convers.*, vol. 24, no. 2, pp. 529–538, Jun. 2009.
[39] R. Dey and S. Nath, "Control and management of different frequency active and reactive powers for multifrequency microgrid," *IEEE Access*, to be published.
[40] II. Buchmann. (2003). *Bu-808: How to Prolong Lithium-Based Batteries*. How to Prolong Lithium-Based Batteries-Battery Univ., Cadex Electronics Inc., [Online]. Available: batteryuniversity.com/learn/article/how_to_prolong_lithium_based_batteries

RAJDIP DEY (Student Member, IEEE) received the B.Tech. degree from the National Institute of Technology, Durgapur, West Bengal, India, in 2014, and the M.Tech. degree from the Indian Institute of Technology Guwahati, Guwahati, Assam, India, in 2016, where he is currently pursuing the Ph.D. degree in electrical engineering with the Department of Electronics and Electrical Engineering.

His research interest includes the analysis and control of multifrequency microgrid.

SHABARI NATH (Member, IEEE) received the B.E. degree in electrical engineering from Rajiv Gandhi Proudyogiki Vishwavidyalaya, Bhopal, India, in 2005, the M.Tech. degree in electrical engineering from the Indian Institute of Technology Bombay, Mumbai, India, in 2008, and the Ph.D. degree in electrical engineering from the University of Minnesota, Minneapolis, MN, USA, in 2012.

Since 2014, she has been an Associate Professor with the Department of Electronics and Electrical Engineering, Indian Institute of Technology Guwahati, India. Prior to that, she was a Product Design Engineer with Cummins Inc., Columbus, IN, USA, for two years. Her research interests include multiport converters, solid-state transformers, power electronic converters for renewable energy systems, and smart microgrids.